Case Studies in Thermal Engineering 9 (2017) 79–89

Contents lists available at ScienceDirect

Case Studies in Thermal Engineering

journal homepage: www.elsevier.com/locate/csite

Enhancement of heat transfer in six-start spirally corrugated tubes

Hyder H. Balla

Al-Furat Al-awsat Technical University, Engineering Technical Collage Najaf, Iraq

ARTICLE INFO

Keywords:
Enhancement of heat transfer
Spirally corrugated tube
Six–starts
Friction factor

ABSTRACT

The utilization of corrugation for improvement in heat transfer is increasingly becoming interesting recently due to its combined advantages such as extended surfaces, turbulators as well as roughness. This study employed the use of both numerical as well as experimental settings on the water flowing at lower Reynolds numbers in a corrugated tubes with spiral shape to evaluate the performance of heat in a newly designed corrugation style profile. The total performance of the heat for the corrugation tubes were determined and the mathematical information generated from both the Nusselt number and the factors of friction were equated with those of the experimentally generated outcome for both standard smooth as well as the corrugated tubes. Analysis of the dat generated revealed improvements in heat transfer ranges of (2.4–3.7) times those 0btained from the smooth tubes with significant increase in the friction factors of (1.7–2.3) times those of the smooth tubes. Based on the findings of study, it was concluded that for extended period and extensive range use, tubes with severity index values at 36.364×10^{-3} could produce better heat performance (1.8–3.4) at Reynolds numbers ranging from 100 to 1300. This was an indication that the geometric expression with spiral corrugation profile could significantly enhance the efficiency of heat transfer with significantly increased friction factors.

1. Introduction

Optimal heat transfer could be obtained by fundamental techniques. These include the passive, active and the compound techniques [1]. While modifications on surfaces, insert or additive are required in the passive technique: an external source is essential in the active technique. The compound technique, as indicated by the name, involve the mixture of either the previous main techniques (passive and active) or it's neither active nor passive but somewhat amid the two techniques, as can be seen in vibrated flow (active) using corrugated tubes (passive) or in electrostatic fields (which is active) using nano-fluids (which is passive) [2]. However, owing to the overwhelming degree in the loss of energy in addition to the quest for small sizes and more economical enhanced thermal transfer device, these 3 techniques have been employed in thermal exchangers and other applications that are relatively related [3]. The main reason for employing heat transfer enhanced techniques is for cutting costs as well as for practical purposes. The major roles of corrugations is for enhancing the secondary re-circulation flows, via induction of the component the radial velocities as well as the mixing of the flow layer. These techniques have been widely utilized in recent heat exchangers [4]. The outcome generated from the surface area modifications or the manipulations of heat transfers, which has been demonstrated to induce swirls or spirally flowing patterns has attracted increasing interests [5]. Additionally, corrugation enhances heat transfer owing to the existence of mixing fluids generated through separations and re-attachments [6]. In an experimental study conducted recently on water and SiO_2 flow in a single plain tube having 5 tubes corrugated at varying height and pitch in corrugation tubes [7] to determine the effect of nano-fluids and corrugations on the rate of heat transfers and pressure drops. The authors of the said experiment reported by increasing the corrugation heights with a corresponding reduction in corrugation pitch could lead to enhancement in heat transfers and consequently causing intensified effects on the nano-particles of the heat transfers. In spirally

http://dx.doi.org/10.1016/j.csite.2017.01.001
Received 25 December 2016; Accepted 3 January 2017
Available online 03 January 2017

Nomenclature

C_p	Heat Capacity at Constant Pressure
D	Tube inside Diameter
E	Error
e	Roughness Height
f	Friction Factor
F_s	Safety Factor
GCI	Grid Independence Index
Gz	Graetz Number
h	Heat Transfer Coefficient
k	Thermal Conductivity
L	Tube Length
m	Slope
Nu	Nusselt Number
P	Pressure
p	Pitch of Corrugation
Pr	Prandtl Number
q″	Heat Flux Per Unit Area
r	Refinement Ratio
Re	Reynolds Number
T	Temperature
u	Fluid Velocity
x	Axial Direction

Greek symbols

μ	Dynamic Viscosity
ν	Kinematic Viscosity of The Fluid
ρ	Density of Fluid
φ	Severity Index, $\varphi=e^2/(pD_n)$
η	Thermal Efficiency

Subscripts

*	Dimensionless
b	Bore
B	Bulk
c	Corrugated
en	Envelope
in	Inlet
n	Nominal
s	Smooth
x	Local

corrugated tube, the flowing of water were also investigated experimentally for the purpose of evaluating characteristic effect of corrugation on lowering pressure and heat transfers at Reynolds number ranging from 17×10^3 to 58×10^3 with the tubes having p (corrugation pitch) of 10 mm and e (corrugation height) of 0.8 mm. The authors of the said study reported that the friction factors ranged from 4 to 5 times greater compared to those from smooth tubes, and the total heat performance of the corrugation tubes was 1.27 greater compared to those from plain tubes [8]. Laminar flowing oils on circular ducts of axial corrugations which are fixed with center-cleared tape that was twisted at Reynolds numbers ranging from 2×10^2 to 8×10^3 has been experimentally investigated [9] determine the friction factors and Nusselt numbers in tubes with p/e=2.0437–5.6481. The findings of these authors revealed that the center-cleared tape that was twisted and axial corrugations produced superior performance compared to those individually used through specific values of center-clearance. Additionally, the increase in the range of heat transfers were in the range of 15–30% consistent pumping power, with a decline ranging from 15% to 25% pumping power for consistent thermal duty. Fluids flowing at Reynolds number ranging from 10^6 to 10^8 in corrugation tubes having p/D=0.886–1.158 and e/D=0.0572–0.0267 has been also investigated [10]. The authors of the said study documented that corrugation heights have significant effects on enhancement of heat transfers, and increasing the corrugation heights consequently lead to reduction in Nusselt number when the Reynolds number is below the vital limits. However, increasing the corrugation heights could be beneficial in improving heat transfers if the Reynolds number is above the vital limits. Flowing of water through corrugation tube of $0.103\le e/D\le0.148$ and $0.462\le p/D\le0.270$ at Reynolds numbers ranging from 10^3 to 10^5 was studied in a previous experiment [11] for the determination of friction factor. In the said

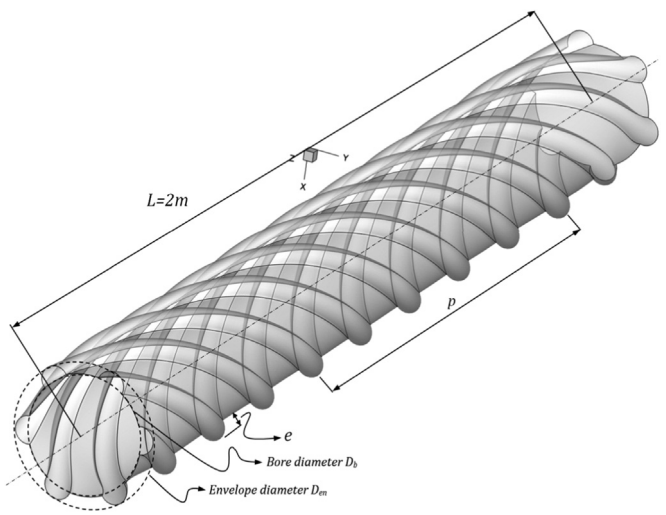

Fig. 1. Six–starts spirally corrugated tube.

study, variations in thermo-physical properties of water were employed excluding heat conduction and thermal capacity. The findings of these authors indicated minor swirl flows interacted with the core mail flows in the pipes and it induced losses of friction.

Currently, paucity of information exist on studies focusing on thermal performances of spirally corrugated tubes, with special interest on the lack of corrugation effect on heat transfers and flow patterns that might permit the flowing of water at low Reynolds numbers. Numerical studies on enhancing heat transfers in spirally corrugated tubes might serve as important technique that could reduce the current limiting facors on the enhancement of heat transfers and thermal performance which are clearly, the interest of thermal exchanger designers. To fill the gap in the literature, newly designed corrugation with corrugation parameters range of (e=2–6 mm and p=10–20 mm) were employed. We hypothesized that smooth spiral corrugation that is cost effective and small sizes may significantly enhance heat transfers and thermal performance with minimised drop in pressure. Fig. 1 showed the adopted stainless steel tubes of six-start corrugation ridings of 2 m in length, having immovable base diameter D_b and adjustable envelope diameter D_n, SolidWorks Softwares was used in conducting this modelings of tube geometries.

This study presents a numerical investigation of spiral corrugations profile in six–start spirally corrugated tubes with a specific range of dimensionless corrugation parameter to study the effects of such corrugation profiles on the improvement of heat transfers and drops in pressure. Additionally, variations in thermo-physical properties of water as the actual case in exchangers, offering outcomes identical to reality was adapted.

2. Geometrical configuration

Corrugated tubes are increasingly becoming more fascinating techniques for acquiring higher efficiency in heat exchangers to minimise costs [12]. Hence, a 1 mm thick aluminum tube of six- start spiral corrugations and one smooth tube was modeled using configurations based on SolidWorks software package. The primary corrugation parameters are the corrugation height (e) and corrugation pitch (p). The envelope diameter D_{en} of the tubes vary depending on corrugation heights e, and fixed bore diameter D_b of 13 mm, as presented in Fig. 1. For the 5 tubes used, each having classical parameters of spiral corrugations with heights to diameter e/D_n, spiral corrugations with pitch to diameter p/D_n and severity index $\varphi=e^2/(pD_n)$ as presented in the first table (Table 1).

2.1. Governing equations

The equations regulating the flow problems in the vector forms are presented in the mathematical expressions below.
Conservation of mass:

$$\nabla\bullet\rho\vec{V}=0 \tag{1}$$

Momentum equation:

$$\nabla\bullet(\rho\vec{V}\vec{V})=-\nabla P+\nabla\bullet(\mu\nabla^2\vec{V}) \tag{2}$$

Energy equation:

$$\nabla\bullet(\rho\vec{V}C_pT)=\nabla\bullet(K\nabla T) \tag{3}$$

2.2. Mesh quality

The Gambit 2.4.6 environment was employed for the interconnecting activities. A tetrahedral element of constant stress element, having four nodes were used. The elements were expressed in three-dimensional space having 3 grades of freedom for each node. The grades of freedom include the translational degree of freedom in directions such as the X, Y and Z, respectively. The grade of the mesh performs crucial roles in the accurateness and steadiness of the numerical computation. The most important qualities of the meshing qualities are parameters such as how the mesh was skewed, aspect ratios and how smooth is the mesh. Checking the characteristics of the grid is necessary notwithstanding the types of meshing utilised in the domain. Subject to the cell type in the mesh (polyhedral, tetrahedral, hexahedral), diverse quality standards are determined. The most crucial factors that indicate mesh quality are the skewness and the aspect ratio. Veluri [13]. The angle of skewness is known as the angle amid the 2 center point

Table 1
Numerical cases (all dimensions in millimeter).

Tube No.	D_b	D_{en}	D_n	e	p	φ
1	11	15	13	2	20	0.0153
2	10	16	13	3	17	0.0407
3	9	17	13	4	14	0.0879
4	8	18	13	5	11	0.1748
5	7	19	13	6	10	0.2769
6	–	–	13	–	–	Smooth

linings. If the skewness is less than 0.75–0.8 for 3D geometries, the meshing is satisfactory and if it is above 0.85, the mesh is unacceptable [14]. The aspect ratio on the other hand, is a degree of stretching of the cells, and it is referred to as the ratios of the optimum length between the cells centroids as well as centroids' face to the minimal length between cell nodes. The finest aspect ratios is 1.0 and this implies that the square of the cells were nicely fixed or the same edge length at all shapes. The variation in cell size has to be gradual and it has to be below 20% alterations from one cell to the other [15]. Any jump in cell size could lead to very poor and consequently, the solution could be difficult to converge. The node and the quantity of the elements are crucial as they can influence the overall output and the periods of computation and invariably the cost of computations. The greater the mesh elements, the more superior the overall output even though the computational time will be prolonged for the completion of the simulation. At this junction, satisfactory mesh quality would offer better solution for both overall satisfactory outcome and computational time [16]. In the current experiment, skewness, aspect ratios as well as the smoothness were chosen to be 0.8%, 1% and 20% respectively.

2.3. Density of the grid

Mathematical errors resulting from the variations between the precise equation and the discretised equation are solved using CFD code. For consistency in the discretisation scheme, the errors could be minimised by an increase in the density of the spatial grids. Moreover, the adaption of higher grid density in the important domains was to captures the more intricate detail of the flow with local small grid size. The swirl and separations that take place in the secondary flow regime requires fine grid to capture. Therefor, the density of the grid in this experiment was managed to be higher at the important domains, specifically close to the wall and moderate at the core flow regime.

At this point there will be no real trillion-cell CFD dataset. The computer with the software required to run this case simply doesn't exist yet. In this study, we have to generate a "simulated" CFD dataset. In an actual CFD case, additional flow features (smaller scale vortices, boundary-layer separation) could be anticipated with increase in the grid density. Hence, The grid density ranges in the current study were 2677027–3808343 tetrahedral cells. A core i7-4700MQ computer of 2.40 CPU and of 16 GB random memory was designated for the simulation purpose. Inspite of the higher densities of meshing utilised which go together with a penalty of increasing the computational time, the computation precision is more important.

2.4. Boundary conditions

ANSYS FLUENT 14.0 was used for the arithmetic simulations of the 2 m corrugated tubes flow model, the meshes were done utilising Gambit 2.4.6 environment and the information generated was analysed by Tecplot 360 softwares. The Reynolds Number ranged from 100 to 1600, and the heat flux applied was 5000 W/m^2. The temperature of the inlet was adjusted to be consistent at 300 K. The water thermo-physical properties were adjusted to be varying with temperature, as the polynomial equation of the water thermo-physical propertis (μ, cp, k, ρ) was fixed to the Fluent database by edition of the fluid properties. The speed of acceleration and pressure fields were coupled by simplified algorithm. The second-order upwind schemes were utilised.

2.5. Convergence criteria

The primary standards for convergence are the index of the grid convergence and the residual values, which has been previously used by Han et al. [17] and Roache [18].

2.5.1. Grid Convergence Index

The Grid Convergence Index (GCI) offers a even quantification of the convergence for grid refinement investigations [18]. It was centred on the estimation of the fractional errors resulting from generalised Richardson extrapolations (Richardson and Gaunt [19]). The GCI values represent the resolution levels and the extent to which the solution approach the asymptotic values.

$$\left.\begin{aligned} GCI_{21} &= F_s \frac{E_{21}}{r_{21}^{o}-1} \\ GCI_{32} &= F_s \frac{E_{32}}{r_{32}^{o}-1} \end{aligned}\right\} \tag{4}$$

where F_s is the safety factor, E is the fraction errors, r is refinement ratios and o is the order of convergence. The numbers 1, 2, 3... referred to coarse, fine, finer....etc. grids respectively. According to Wilcox [20], the safety factor F_s value is 1.25 for comparisons among more than two grids while for comparisons between two grids, the safety factor F_s value is 3.0.

Three fine mesh spacing of 0.4, 0.3 and 0.2 were tested for the purpose of selecting mesh with better spacing for consistency and precision of the simulations. The selected mesh spacings were true for cells lining next to the walls and as the cell dimension increases from the wall toward the center of the tube at growth factor of 1.2.

The GCI was computed for each mesh spacing and it was found that 0.028 and 0.0471 hold for GCI_{32} and GCI_{21} respectively. From the GCI outcomes, there was a decline in GCI values for consecutive grid refinement ($GCI_{32} < GCI_{21}$) in all the 3 parameters. The GCI values for finer grids (GCI_{32}) were moderately low in comparison to coarser grids (GCI_{21}), an indication that the dependence of the numerical simulations on the size of cell was minimised. In addition, as the decline in GCI values from coarser grids to finer grids is moderately higher, the grid independent solution is likely to have been obtained. At this point, further refinements of the grid would not produce significant alterations in the simulation outcomes.

2.5.2. Residual convergence

The residual constitutes one of the most pronounce quantification of the convergence of iterative solutions, due to the fact that it measures directly, the errors in the solutions of the equation system. In the analysis of CFD, the residual quantifies the resident imbalance of the parameters conserved in individual control volumes. Hence, all cells in a model would possess distinct residual values for every equation resolved.

Residual values usually never attain zero value in iterative geometric solutions. Meanwhile, the lesser the values of the residual, the greater the numerical precision of the solutions. All CFD codes have individual procedures for standardizing the residual solutions. It could be of great interest to monitor the documentation of the code in order to be appropriately guided with standards when convergence are judged.

In CFD codes, residual values of up to 10^{-4} are usually regarded as loose convergence whereas values of up to 10^{-5} are regarded as moderate convergence, and values of up to 10^{-6} are regarded as tight convergence. In this experiment, the equations for residual curves of continuity, energy equations, x-velocity, y-velocity as well as z-velocity were respectively 2.1×10^{-5}, 3.7×10^{-5}, 9.2×10^{-6}, 5.1×10^{-7} and 2.6×10^{-7}.

3. Results and discussion of heat transfer

3.1. Validation of Nusselt numbers

The obligatory convective heat transfers valuation standards in this study was represented by local or mean Nusselt numbers *Nu*. For the purpose of validating the information generated by the simulated smooth and corrugated tubes with those reported in other related experiments, Churchill and Ozoe formulated an equation which takes into consideration both the entrance as well as completely established regions [21] as shown below

$$Nu_x=\left[4.364\left(1+\left(\frac{Gz}{29.6}\right)^2\right)^{\frac{1}{6}}\right]\left[1+\left[\frac{Gz/19.04}{[1+(Pr/0.0207)^{2/3}]^{1/2}[1+(Gz/29.6)^2]^{1/3}}\right]^{3/2}\right]^{1/3} \tag{5}$$

where

$$Gz=\frac{\pi}{4x_*}=\left[(\pi Re_{D_n}\bullet Pr)/4\left(\frac{x}{D_n}\right)\right] \tag{6}$$

The mathematical expression (equation) presented above has a maximal range of deviation up to ± 5% with numerical information in the *Pr* ranging from 0.7 to 10. It also possess consistent asymptotic behaviour of both lesser and larger *Gz* and *Pr* respectively. Another consistent and widely used empirical correlations for flowing of fluids in smooth tube was proposed by Shah and London [22]

$$Nu=\begin{cases}1.953(RePrD/L)^{1/3};(RePrD/L)\geq 33.3\\ 4.364+0.0722RePr\frac{D}{L};\quad (RePrD/L)\leq 33.3\end{cases} \tag{7}$$

where *D* is equivalent to D_n in this experiment.

Abdel-Kariem and Fletcher [23] suggested an emperical correlations for laminar flowing of fluids in corrugation tubes in the expression below

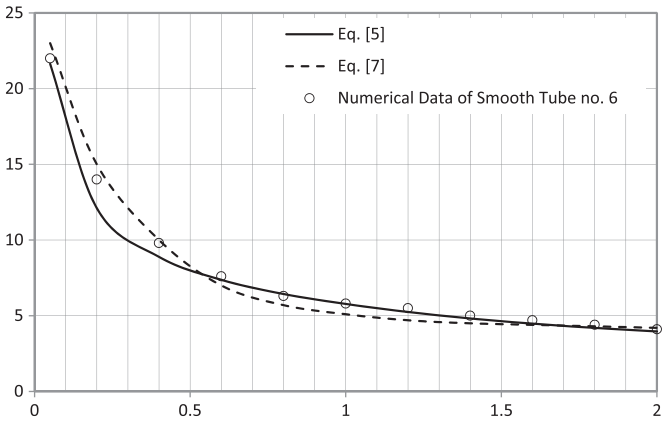

Fig. 2. Validation of Nusselt numbers of smooth tube no. 6 with Eqs. (5) and (7).

$$Nu=0.\ 777Re^{0.444}\left(\frac{\theta}{45}\right)^{0.67} \tag{8}$$

where θ is the helix angle of the corrugation in measured degrees

The equation above was found to correlate at $70\leq Re\leq 12\times 10^2$, and the range of Reynold number was almost identical with the current Re range.

Smooth tubes of the Eqs. (5) and (7) which are widely employed and they had been utilised for confirmation purposes in several studies [24,25] were used for the validation. The numerical information generated by the Nusselt numbers in the non-corrugated tubes no. (6) was likened to both Eqs. (5) and (7) as presented in Fig. 2. A credible outcome was obtained with the maximal deviation below ± 2%, ± 3% and ± 1.5% respectively. These deviation range were acceptable based on reports documented in a related heat transfers improvement experiment conducted by Balla [25]. The observed deviation was an indication of the appropriateness of the mesh density utilised, and the predicted convergence standards fall within the safe side. Zero error process is usually absent in numerical investigations. However, errors from simulated parameters are commonly available for several reasons. For instance, whatever could the iteration number be, the residual of convergence does not usually get to zero, hence deviations will still be available. The variation between Eqs. (5) and (7) and other numerical results probably came up as a result of the fact that these equations were derived from different valuses of p/D_n and e/D_n, with varied corrugation profiles. The reasons presented are highly crucial in enhancing heat transfers and any little alterations in these values, would lead to emergence of a remarkable results. Additionally, the effects of Prandtl number does not account for the stated correlations, that make the deviation large.

3.2. Heat transfer results

When analyzing the flow patterns, CFD codes performs an essential and overwhelming role, and the details of the small flow qualities such as the secondary swirl flow and the vorticities could be accounted by the CFD simulation. Significantly increased rate of thermal transfer could be induced by the variations temperature between the wall and the bulk temperature, for instance, the tube with highest ΔT is the tube with higher rate of thermal transfer. It could be deduced from Fig. 3 that tube no. 5 with severity index value of 0.2769 has the greatest difference in temperature, while the lowest difference in temperature was obtained from tube no. 1 with severity index of 0.0153. The differences in temperature was attributed to the mixing of fluid layers at the secondary region induced by corrugation, and as the corrugation becomes severe, the mixing will also increase.

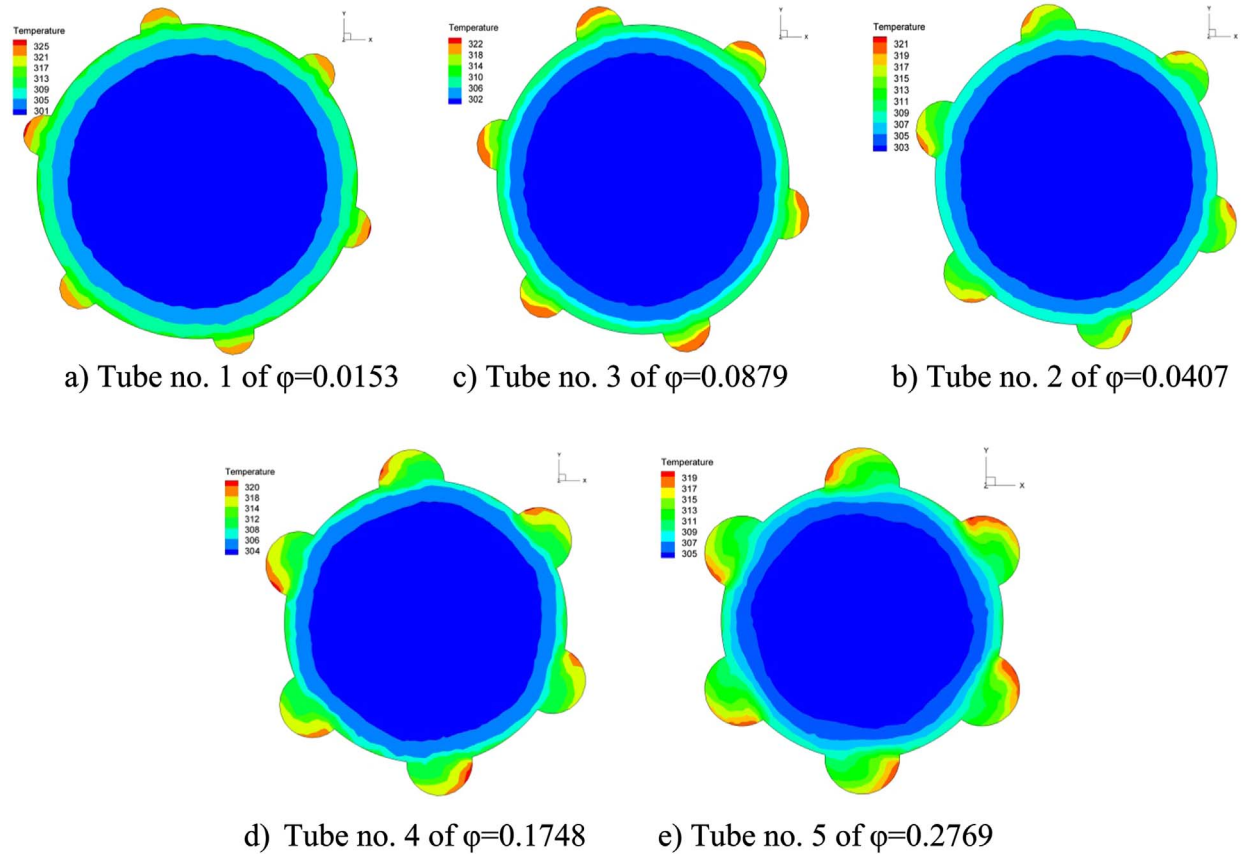

Fig. 3. Temperature contour.

Figs. 4((a)–(e)) and 5((a)–(e)) present the velocity vector and streamlines respectively of the corrugated tubes upon which the effects of severity index could be clearly noted. The tube of low severity index (tube no. 1) was found to have low degree of turbulence at the secondary flow region and the core flow had relatively medium velocity. As the severity index increases, the difference in velocities between fluid layers which were adjacent to the wall and the core flow layers became bigger as observed in tube no. 5. This behavior was attributed to the periodic mixing of flow fluid to the core.

The extent of improvement could vary depending on the extent of variations in the index of the severity since the corrugation produces swirls that distort the heat and hydraulic boundary layers and this heat transfers mechanisms has been previously reported [5].

Fig. 5 presents the comparison between local Nusselt numbers (Nu_x) and inversed Graetz numbers (Gz^{-1}) which is a function of (Pr, Re, and x/D_n) as it was depicted in Eq. (6), where the Nu_x is not indirectly proportional to the Gz^{-1}. The figure provides an evidence showing that enhancement in the Nu_x was significantly increased as φ increase.

Fig. 6 presents the numerical Nu versus Re for differences in severity index φ as well as the validation of the Nusselt number in tube no. (6) with Eq. (7).

As earlier stated, severity is the combination of the effects of all the parameters of corrugation into a single equation excluding the effects of convective surface areas which could be inferred from the improved Nu data. The figure indicates a rapid increase in Nu as φ increases owing to the alterations in the boundary layers through the severity of the roughness. The corrugation used operated as a swirl enhancer for the fluids layer that were in connection with the walls of the tube and putting them together with the major flow. This led to enhancement of heat transfers. It is worthy of mentioning that Fig. 7 indicates enhancement in heat transfers ranging from 2.4 to 3.7 times those of smooth tubes.

The pressure drop along the tube is significantly increases as severity index increase. This is normal behavior due to the obstacles increase (corrugation) as shown Fig. 7((a)–(e)).

3.3. Validation of pressure drop

The friction factor f as it represent the drop in the pressure was calculated for the whole dimension of the tubes, the laminar faning friction factors were provided via the mathematical expression below

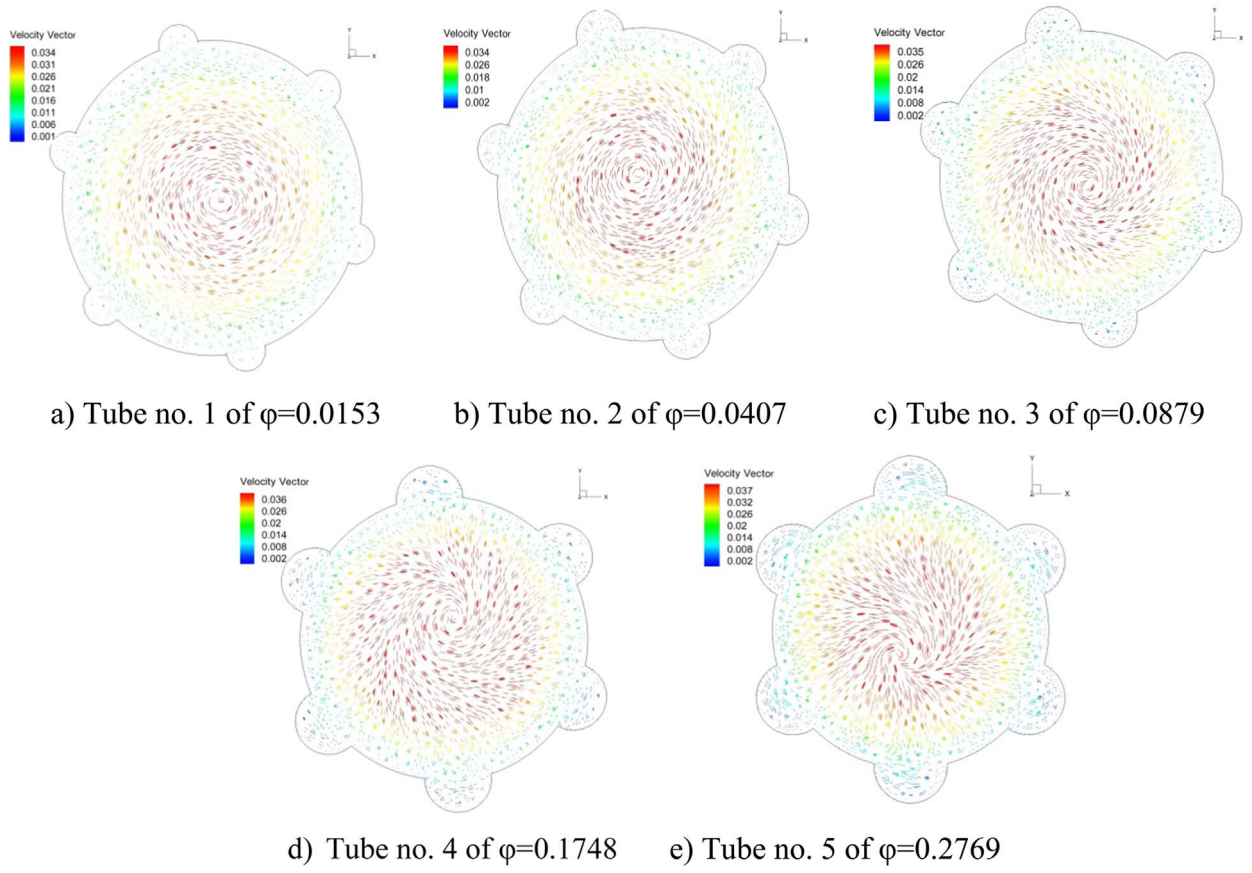

Fig. 4. Velocity vector.

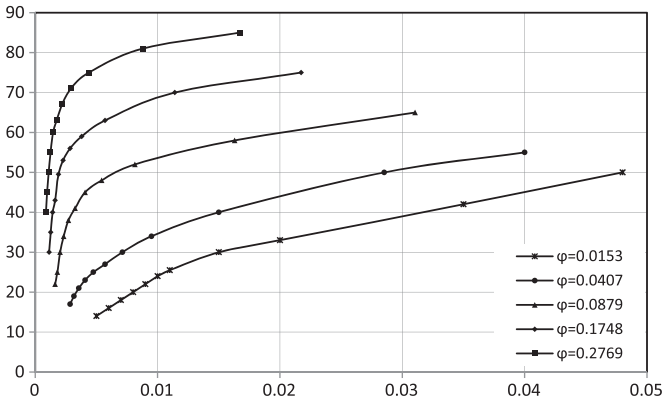

Fig. 5. Nusselt Nu_x number versus Graetz number Gz^{-1} for differences in Severity values.

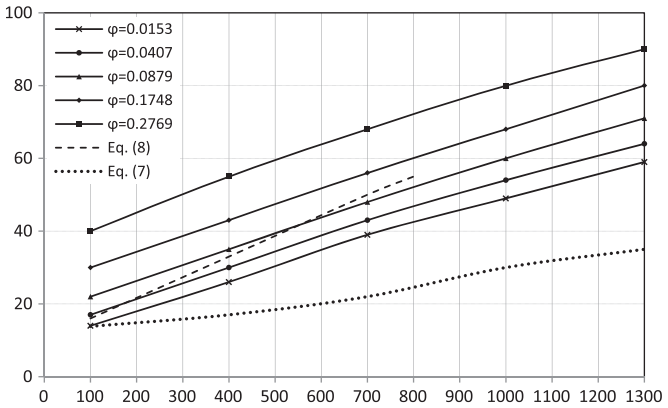

Fig. 6. Mean Nusselt *Nu* numbers versus Reynolds numbers *Re* for differences in the value of Severity index φ.

$$f=16/Re \tag{9}$$

A wide range ($5\times10^2 \le Re \le 5\times10^4$) of correlations for flowing oils and water in elliptical axis tubes with p/D=2–3 has been proposed [26]. Their correlations is presented in the mathematical expression below

$$f=1.\ 54Re^{-0.32} \tag{10}$$

The confirmation of the friction factors for the numerical outcome of the smooth tube no. 6 with Eq. (9) was shown in Fig. 8. Additional refinement of the grid and manipulations of the mesh spacing were found to play significant function in reducing the deviations associated with the validated findings obtained. Additionally, the adopted second-order upwind schemes pushed the results of the simulation almost identical with results obtained from experiments. These factors entirely contributed in reducing the errors associated with numerical simulations. Hence, maximal deviation of ± 1% was observed. The deviation of Eq. (10) was acceptable due to the fact that it holds for corrugated tubes, and the curves were normal with regard to the effects of corrugations in friction factors. Generally, comparing parameters in this figure provide credible consistency and reliability to the data generated from this study. However, we have to mention that the deviations in CFD codes also occurred owing to the fact that the residual convergence could sometimes be attained, but the curve of the wall temperature may yet be unstable and this is an indication that the fluid does not transferred the optimal quantity of heat to the walls. The thermal equilibrium between the wall and bulk temperatures has to be achieved before ending the iteration solutions to obtain pricise value.

Fig. 9 shows significant value of *f* with reference to what has been reported in other studies and this could be as a result of adopting successive as well as smooth curvy corrugations that provides widespread surface area, leading to decline in flow retarding with immovable throat cross-sectional areas. Furthermore, the geometric corrugations used produce coherence and logical swirls at secondary flow regions that helped in reducing the drop in pressure at the same time preserving the pumping power. Apparently, when p/D_n is reduced, e/D_n will increase, implying, increase in φ would lead to increase in friction factor at steady Re for 2 major explanations. Firstly it is denoted by the rise in the wet perimeters, implying greater dimensions cleared by the working fluids. Secondly, it is signified by the collisions among fluid particles as a result of curvatures. But, the extent to which the friction factor might be increased depends on the nature of the corrugation profile adopted, styles and parameters.

From the above figure, as φ increase, the *f* also increased as a result of the rise in the severity of roughness (pitch and depth) that makes the swirls stronger, generating greater frictions among the working fluids and the wall of the tube. Other credible explanation on the observed loss of power could be the perpendicular constituents of the rate trajectory (radial velocity components) to the

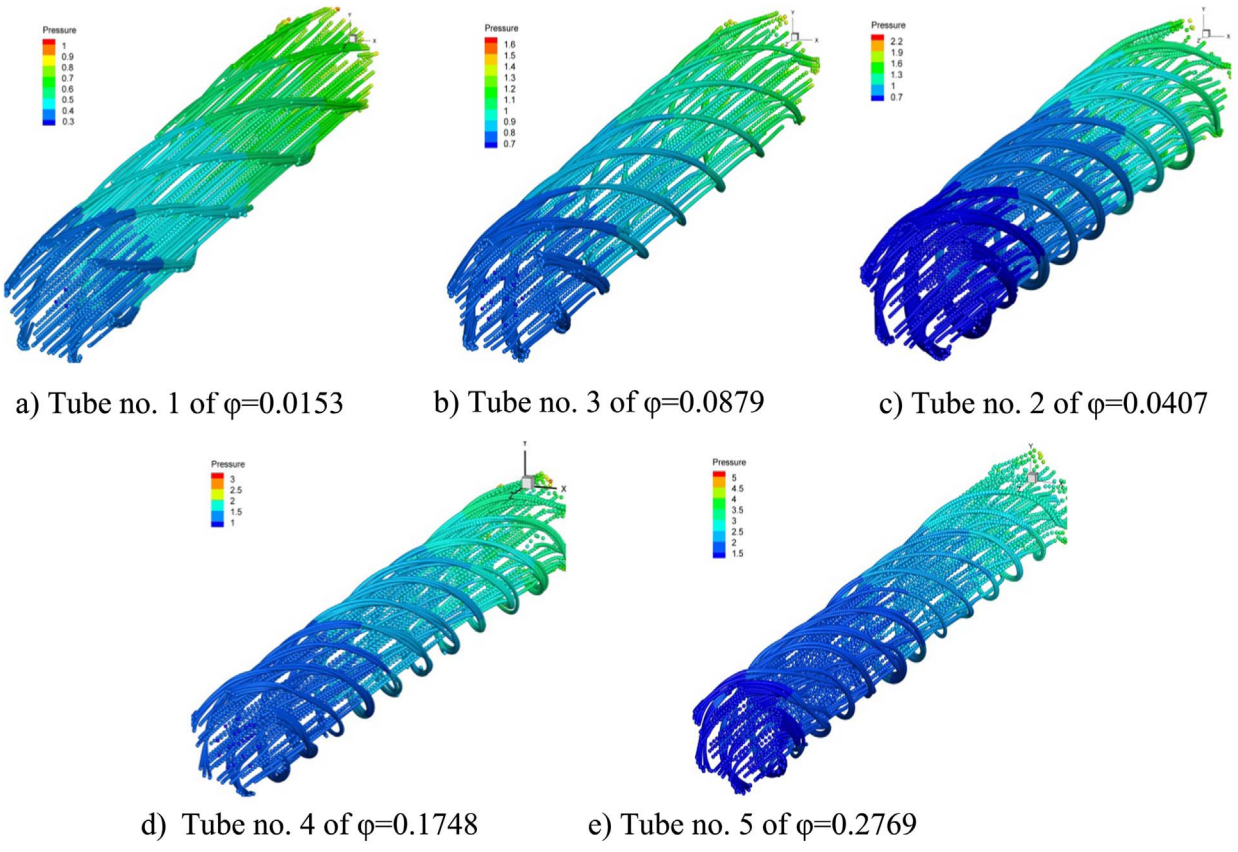

Fig. 7. Pressure drop contour.

direction of the major flow produces substantial impediment, its effects increases as φ is raised. The increase in frictional factor were found to range from 1.7 to 2.4 times those of smooth tubes.

4. Performance criteria

Efficient evaluation of improved surface is a cost effective criterium, and it is the main criterium for thermal enhancement. But, thermal and hydraulic criteria need to be equally taken into consideration. Webb [27] proposed that the primary variables that are influential include pressure drop, rate of thermal transfer as well as rate of flow for archiving optimal surface geometries for flows in the tubes.

The applicability and reliability of these criteria which has been utilised in many experiments is the efficiencies of thermal performance. It signifies the heat transfers coefficient ratios of the improved tubes with promoters of non-corrugated tubes at steady

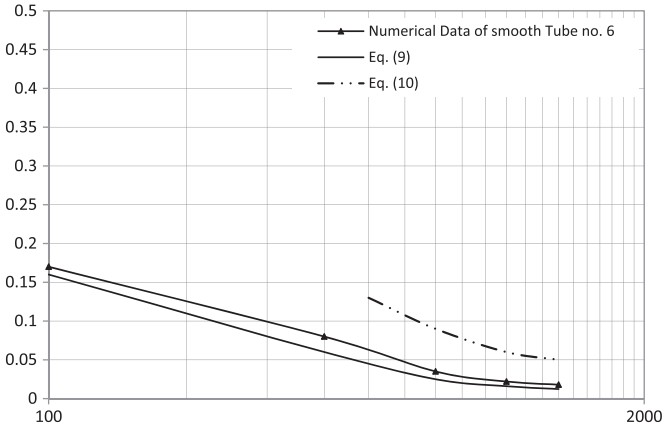

Fig. 8. Friction factor validation.

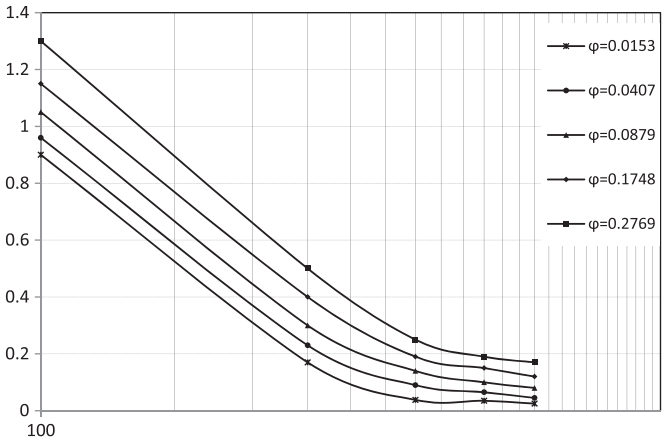

Fig. 9. Friction factor versus Reynolds number.

pumping power [28].

$$\eta = (Nu_c/Nu_s)/(f_c/f_s)^{1/3} = f(Re_s) \tag{28}$$

Fig. 10 presents the thermal efficiency against *Re* for differences in the value of φ, it revealed that φ is directly proportional to increase in *Re* through the value of *Re*≈600. This implied that the heat acquired was greater compared to the rise in friction, and the severity appeared to possess inverse function effects, and the condition lasted through *Re*≈800.

Later, the normal relation of inverse proportion of φ with Reynolds number was retrieved as a result of the rise in frictional factors, becoming higher in comparison to the enhancement on heat transfers when the flow approached regions of transition. Hence, effects of friction could overwhelm effects of thermal transfer acquired as indicated in the curve patterns. The low severity tube was found to performs better compared to the performance of high severity tubes. For prolonged and extensive use, tubes with high severity has to be used, and for this study, a tube with value of severity 0.2769 was found to produce the greatest thermal performance of 1.8–3.4 for *Re*=100–700 and η=2.6–3.4 for *Re*=700–1300.

5. Conclusion

A six–start spirally corrugated tube was evaluated numerically to quantify the effects of newly designed spiral corrugations with characteristics such as e/D_n and p/D_n signified by a parameter known as severity index φ on total heat performance.

Analysis of the results revealed that the adoption of the geometry used with smooth spiral corrugation could significantly enhance heat transfers ranging from 2.4 to 3.7 times those from non-corrugated tubes with significant rise in frictional factors ranging from 1.7 to 2.4 times those from non-corrugated tubes. The greatest thermal performance in the range of 1.8–3.4 was found to belong to the tubes with φ values of 0.2769 at *Re*=100–700, and η=2.6–3.4 for *Re*=700–1300. Based on these findings, we opined that the best way to enhance heat transfers while maintaining least pressure drop is the use of corrugation profiles. However, the parameters need to be to be adjusted for these purposes. Furthermore, our findings showed that severity index φ has greater effects on enhancement of heat transfers and frictional factors, and the heat acquired was associated with loss of pressure, specifically at higher

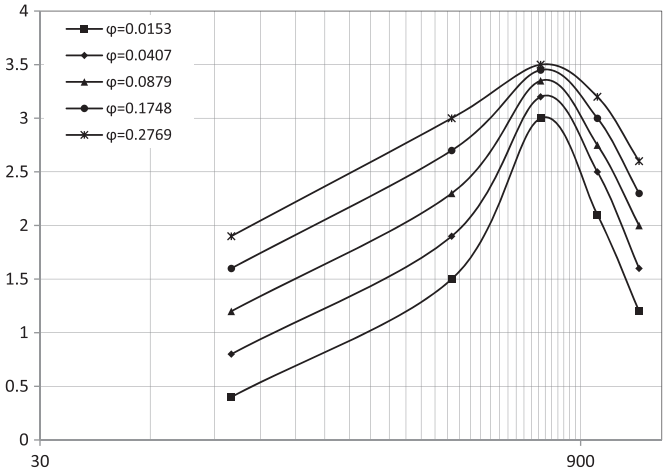

Fig. 10. Thermal performance factor versus Reynolds number.

Re. Additionally, it was concluded that adoption of corrugation profiles could produce coherence and systematic swirls at secondary flow regions that could reduce sufficiently, the loss of pressure while preserving the pumping power.

References

[1] Z.S. Kareem, M.N. Mohd Jaafar, T.M. Lazima, S. Abdullahb, A.F. Abdulwahida, Passive heat transfer enhancement review in corrugation, Exp. Therm. Fluid Sci. 68 (2015) 22–38.
[2] S. Liu, M. Sakr, A comprehensive review on passive heat transfer enhancements in pipe exchangers, Renew. Sustain. Energy Rev. 19 (2013) 64–81.
[3] S.V. Patil, P.V.V. Babu, Heat transfer augmentation in a circular tube and square duct fitted with swirl flow generators: a review, Int. J. Chem. Eng. Appl. 2 (2011) 326–331.
[4] S. Rainieri, G. Pagliarini, Convective heat transfer to temperature dependent property fluids in the entry region of corrugated tubes, Int. J. Heat. Mass Transf. 45 (2002) 4525–4536.
[5] H. Wu, H. Cheng, Q. Zhoum, Compound enhancement heat transfer inside tubes by combined use of spirally corrugated tube and inlet axial vane swirlers, Enhanc. Heat. Transf. 7 (2000) 247–257.
[6] S.K. Saha, Thermohydraulics of laminar flow through a circular tube having integral helical corrugations and fitted with helical screw–tape insert, Chem. Eng. Commun. 200 (2013) 418–436.
[7] A.A.R. Darzi, M. Farhadi, K. Sedighi, R. Shafaghat, K. Zabihi, Experimental investigation of turbulent heat transfer and flow characteristics of sio_2/water nanofluid within helically corrugated tubes, Int. Commun. Heat. Mass Transf. 39 (2012) 1425–1434.
[8] Uhia, F.J. Fernandez-SearaJ, Heat transfer and friction characteristics of spirally corrugated tubes for outer ammonia condensation, Int. J. Refrig. 35 (2012) 2022–2032.
[9] S.K. Saha, B.N. Swain, G.L. Dayanidhi, Friction and thermal characteristics of laminar flow of viscous oil through a circular tube having axial corrugations and fitted with helical screw-tape inserts, J. Fluids Eng. 134 (2012) 051210.
[10] F. Wu, W. Zhou, numerical simulation and optimization of convective heat transfer and pressure drop in corrugated tubes, Heat. Transf. Res. 43 (2012) 527–544.
[11] C.O. Popiel, M. Kozak, J. Małecka, A. Michalak, Friction factor for transient flow in transverse corrugated pipes, J. Fluids Eng. 135 (2013) 074501.
[12] S.J. Kline, F.A. McClintock, Describing uncertainties in single-sample experiments, Mech. Eng. 75 (1953) 3–8.
[13] S.P. Veluri, Code Verification and Numerical Accuracy Assessment for Finite Volume CFD Code (Ph.D. Thesis), Virginia Polytechnic Institute and State University, USA, 2010.
[14] R. Zhang, Y. Zhang, K.P. Lam, D.H. Archer, A Prototype mesh generation tool for CFD simulations in architecture domain, Build. Environ. 45 (2010) 2253–2262.
[15] A. Skoglund, Preservation of Wakes in Coarse Grid CFD (M.Sc. Thesis), Chalmers University of Technology, Sweden, 2008.
[16] M.M. Noor, A.P. Wandel, T. Yusaf, Detail guide for cfd on the simulation of biogas combustion in bluff-body mild burner, in: Proceedings of the ICMER Conference, Kuantan, Malaysia, 2013.
[17] H. Han, B. Li, B. Yu, Y. He, F. Li, Numerical study of flow and heat transfer characteristics in outward convex corrugated tubes, Int. J. Heat. Mass Transf. 55 (2012) 7782–7802.
[18] Roache, P.J.,, Perspective: a Method for uniform reporting of grid refinement studies, J. Fluids Eng. 116 (1994) 405–441.
[19] L.F. Richardson, J.A. Gaunt, The deferred approach to the limit. Part I. Single Lattice. Part II. Interpenetrating Lattices, Philos. Trans. R. Soc. Lond. 226 (1927) 299–361.
[20] D.C. Wilcox, Turbulence Modeling for CFD, third ed., PratyushPeddireddi, Calfornia, 2006.
[21] A. Bejan, Forced convection: internal flow, in: A. Bejan, A.D. Kraus (Eds.), Heat Transfer Handbook, John Wiley & Sons Inc, New Jersey, 2003, pp. 5.411–5.413.
[22] R.K. Shah, A.L. London, Laminar Flow Forced Convection in Ducts, first ed., Academic Press, Massachusetts, 1978.
[23] A.H. Abdel-Kariem, L.S. Fletcher, A Comparative analysis of heat transfer and pressure drop in plate heat exchangers, in: Proceedings of the Fifth ASME/JSME Thermal Engineering Conference, California, USA, 1999.
[24] T.M. Lazim, Z.S. Kareem, M.N. Mohd Jaafar, S. Abdullah, A.F. Abdulwahid, Heat transfer enhancement in spirally corrugated tube, Int. Rev. Model. Simul. 7 (2014) 970–978.
[25] H.H. Balla, S. Abdullah, R. Zulkifli, W.M. Faizal, K. Sopian, effect of oxides nanoparticle materials on the pressure loss and heat transfer of nanofluids in circular pipes, J. Appl. Sci. 12 (2012) 1396–1401.
[26] J. Meng, X. Liang, Z. Chen, Z. Li, Experimental study on convective heat transfer in alternating elliptical axis tubes, Exp. Therm. Fluid Sci. 29 (2005) 457–465.
[27] R.L. Webb, Performance evaluation criteria for use of enhanced heat transfer surfaces in heat exchanger design, Int. J. Heat. Heat. Mass Transf. 24 (1981) 715–726.
[28] H. Han, B. Li, H. Wu, W. Shao, Multi–objective shape optimization of double pipe heat exchanger with inner corrugated tube using RSM method, Int. J. Therm. Sci. 90 (2015) 173–186.